scientific reports

OPEN

Effects of cation types on physicochemical parameters and micro-structure of soft clay for electrochemical treatment

Guohui Yuan[1,2,3], Xiaomeng Cao[4], Ziyang Gao[1,2], Junfeng Ni[1,2], Xiaobing Li[1,2✉], Hongtao Fu[1,2], Jianqi Wu[3,5] & Chenyang Zhou[3,5]

To investigate the influence of cations on the microstructural characteristics of electrochemical reinforcement in soft clay, a study was conducted using three different cationic salt solutions—NaCl, CaCl₂, and FeCl₃—for grouting treatment. Four sets of indoor experiments were performed to examine the reinforcement mechanism of the electrochemical method. The findings indicate that increasing the valence of injected cations significantly affects the electrochemical reinforcement effect and the soil's microstructural properties. Higher-valence cations notably enhanced the soil's electrical permeability coefficient and conductivity, leading to a substantial improvement in shear strength. Furthermore, the pore volume of the soil increased following electrochemical treatment compared to soil treated solely by electro-osmosis, due to the flocculation effect induced by cation injection. Nevertheless, the pore size distribution became more uniform, especially in the cathode region, as a result of pore redistribution. The chemical cementation reactions triggered by Ca^{2+} and Fe^{3+} injections mitigated the impact of flocculation on the microstructure, resulting in a more favorable pore volume and size distribution compared to Na^+ treatment.

Keywords Electrochemical, Soft clay, Microscopic pore structure, Electric permeability coefficient, Consolidation

Electro-osmosis is a method that utilizes a direct-current (DC) electric field to enhance soil drainage and reinforcement. Compared to traditional soft clay drainage consolidation methods, such as preloading method and vacuum preloading, electro-osmosis provides faster reinforcement, better effectiveness in deep soils, and is not limited by permeability[1]. In addition, this method can remove weakly bound water from the soil, making it particularly suitable for reinforcing low-permeability soils with a high content of fine particles[2–4]. The electroosmosis method was first successfully applied in engineering practice by Casagrande[5]. Since then, its research and application have expanded significantly.

The electrokinetic consolidation of soil is a very complex process, including electro-osmosis, electrophoresis, electrolysis, and ion transportation[6]. The electroosmosis reinforcement effect can be divided into two main components: drainage consolidation and chemical reinforcement. Chemical reinforcement occurs when metal cations present in the soil, along with those released through electrode corrosion, migrate toward the cathode under the influence of the DC electric field. In the alkaline environment near the cathode, these cations react to form cementation precipitates, which further enhance soil strength[7–9]. Based on the theory of chemical reinforcement of soil, Bjerrum[10] combined chemical grouting with electroosmosis method, achieving superior reinforcement results. Since then, the electrochemical method has achieved superior reinforcement results[11–13].

Existing research on electrochemical methods primarily focuses on the reinforcement effects of different reagents. Xue[14] analyzed the evolution of soil properties when $Ca(NO_3)_2$ was injected at the anode and Na_2SiO_3 at the cathode, showing that during electro-osmosis, Ca^{2+} migrating to the cathode reacts with OH⁻ and SiO_3^{2-} migrating to the anode, leading to a cementation reaction near the cathode that improves soil strength in that area. The increase in soil strength near the anode was primarily attributed to a decrease in water content.

¹College of Civil Engineering and Architecture, Wenzhou University, Wenzhou, China. ²Key Laboratory of Engineering and Technology for Soft Soil Foundation and Tideland Reclamation of Zhejiang Province, Wenzhou, China. ³Jiangxi University of Science and Technology, Ganzhou, China. ⁴Zhejiang Geology and Mineral Technology Co., Ltd, Wenzhou, China. ⁵Jiangxi Provincial Key Lab of Environmental Geotechnical and Engineering Disaster Control, Ganzhou, China. ✉email: ac-lxb@wzu.edu.cn

1

Otuski[12] used $Mg(CH_3COO)_2$ as the anode solution and Na_2CO_3 as the cathode solution for electro-chemical reinforcement of kaolin, achieving a maximum shear strength of 300 kPa, thereby demonstrating the feasibility of electro-chemical soil reinforcement. Chien[15] injected $CaCl_2$ and Na_2SiO_3 solutions successively into the soil, resulting in an average shear strength increase of 195% near the cathode. Liu[16] discovered that there is an optimal salinity level in the electrochemical reinforcement process, where excessive salinity inhibits electro-osmotic drainage; they also found that $CaCl_2$ provided better reinforcement than KCl and NaCl. Ou[17] conducted a series of comparative experiments and found that the electrochemical strengthening time can be shortened by up to 40% compared with electro-osmosis alone. Paczkowska[18] explored the electro-osmotic effect of methacrylic polycation, finding that the polymer made the water content distribution more uniform by electrochemical reinforcement, and the drainage effect was four times greater than in cases without the polymer. Previous studies have primarily focused on the macro-level differences in the strengthening effects of individual reagents (e.g., $CaCl_2$) or reagent combinations (such as $CaCl_2$ and Na_2SiO_3). However, there is limited in-depth research on electrochemical reinforcement concerning reagents containing the anion (Cl^-) but different cations. Thus, investigating the impact of cation valence on the electrochemical reinforcement of soft clay and its influence on pore characteristics is essential.

Regarding the reinforcement mechanism, scholars have also analyzed the microstructural changes in soil after electrochemical reinforcement. Ou[19] examined the microscopic changes near the cathode after the injection of $CaCl_2$ solution during the electrochemical reinforcement process. Their study showed that the strength improvement of the soil sample near the cathode after electrochemical reinforcement was mainly due to the cementation reaction of Ca^{2+} in a strongly alkaline environment. The microscopic images revealed that the resulting cementing material effectively filled the pores in the kaolin. Chien[20] investigated the impact of reagent injection timing on electrochemical reinforcement, finding that injecting $CaCl_2$ solution at the start of electro-osmosis, followed by Na_2SiO_3 solution when the current decreased and the cathode stopped draining, led to better reinforcement. Microscopic images indicated the presence of distinct cemented areas near the cathode, with smaller pores. Ge[21] combined stabilization/solidification with electrochemical reinforcement, and analysis using scanning electron microscopy (SEM) and mercury intrusion porosimetry (MIP) showed that the combined approach provided better soil reinforcement than either method alone. Korolev[22] studied the effect of electroosmosis on the microstructure of soil, and found that electroosmosis treatment redistributed the size of pores. The pores in the soil are mainly large micropores, with larger micropores having adverse effects on electroosmosis. Mahalleh[23] conducted microstructural and chemical analyses of the soil after electro-osmosis, discovering that the treated soil exhibited agglomeration and precipitates, with a higher concentration of calcium ions in the cathode area. This indicated that electro-osmosis induces ion exchange and migration, promoting the evolution of soil microstructure. While these studies primarily focus on microscopic changes caused by electro-osmosis or a single type of solution, the differences in the effects of various solutions on the microstructure during electrochemical reinforcement are rarely addressed.

It can be seen from the above studies that there is a lack of studies on the selection of electrochemical solutions and the microscopic changes brought by different types of solutions. To address this, the present paper investigates the influence of cation types on the electrochemical consolidation of soft clay. Salt solutions with varying cationic valence were injected into soft clay to analyze the changes in current, temperature, water content, and shear strength. Additionally, the microstructural characteristics of the soil before and after treatment with different cation salt solutions were compared to assess the effect of cations on electrochemical consolidation. This research aims to provide valuable insights for selecting appropriate reagents in the practical application of electrochemical methods.

Test methods and materials
Soil sample
The test soft clay originated from the Dongtou reclamation area in Wenzhou, Zhejiang, China, the physical properties of the soil sample are shown in Table 1.

Experimental apparatus
The schematic diagram of the experimental apparatus, made from plexiglass, is shown in Fig. 1. The electro-osmosis cell is divided into three parts by two plexiglass plates with a bottom opening. The middle compartment (500 mm×200 mm×200 mm) is used for the soil sample, and the two outside compartments (50 mm×200 mm×200 mm) serve as drainage channels. A GWSPD-3606 regulated DC power supply

Physical and chemical properties	
Water content (%)	78
Specific gravity of soil	2.75
Void ratio	1.68
Plastic limit (%)	25.4
Liquid limit (%)	52.1
Undrained shear strength (kPa)	≈0
pH	7.4

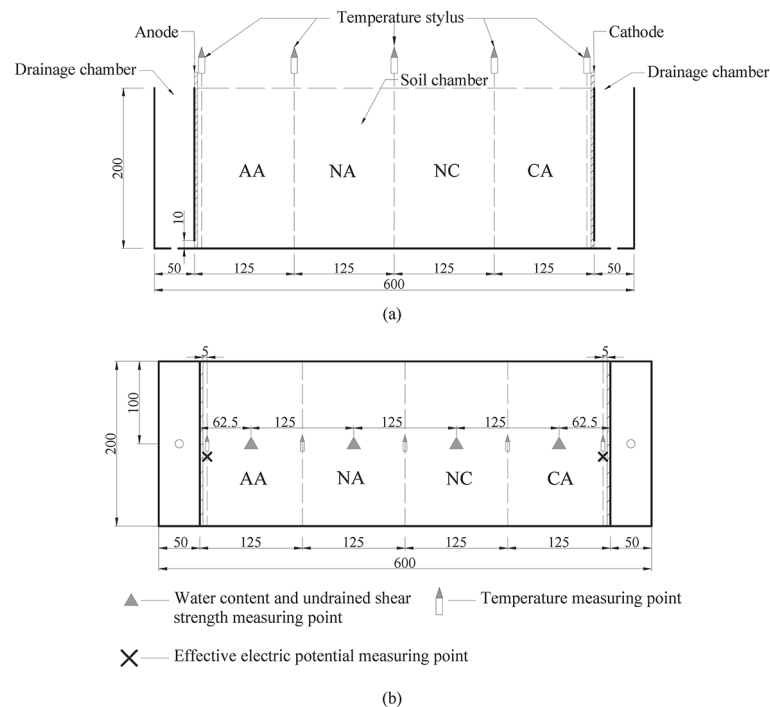**Table 1.** Physical and chemical properties of soil sample.

Fig. 1. Schematic of test apparatus (**a**) Profile view (**b**) Plan view

Test	Chemical solution	Concentration	Injection volumes	Potential gradient
T0	Deionized water			
T1	NaCl	0.5 mol/L	100mL	1 V/cm
T2	CaCl$_2$			
T3	FeCl$_3$			

Table 2. Test Schemes.

was used to generate the DC electric field. To prevent the cations produced by electrode corrosion from affecting the experimental results during the electroosmosis process, the electrode was made of graphite(200 mm×200 mm×4 mm), The cathode surface was perforated with evenly distributed 5 mm diameter holes to facilitate drainage. During the test, the electrode plates were placed at both ends of the soil sample compartment, and geotextiles were placed on the side of the electrode facing the drainage compartments to prevent the loss of soil samples. Temperature and electric potential probes were inserted into the soil sample to monitor the effective potential and temperature changes throughout the test. The positions of the measuring points are shown in Fig. 1b.

Test procedure

Four experiments were conducted in this study, with T0 serving as the electro-osmotic control group and T1-T3 representing the electrochemical groups. In the T1-T3 experiments, solutions of NaCl, CaCl$_2$, and FeCl$_3$, each at the same concentration, were injected into the soil, as detailed in Table 2. To ensure uniform diffusion of the solutions, the reagents were mixed into the soil samples and allowed to stand for 24 h before testing began. An equal volume of deionized water was added to the T0 group to account for any variations caused by additional water injection. The soil chamber's inner surface was coated with Vaseline, and electrodes were placed at both ends of the model box, with geotextiles attached to the sides of the electrodes facing the drainage chambers to prevent soil loss. The slurry was poured into the soil chamber in layers, using a vibrating machine to eliminate air bubbles. The portable temperature probe used during the experimental testing is the TM-6801 model. Temperature and potential probes were positioned according to the measuring points shown in Fig. 1b. A voltage gradient of 1 V/cm was applied using direct current, and drainage volume, current, temperature, and effective electric potential were recorded at intervals: every 0.5 h for the first 2 h, every hour between 2 and 4 h, every 2 h between 4 and 20 h, and every 4 h thereafter. Energization was stopped when the drainage rate fell below 5 mL/h in all tests to ensure consistent energization times. Following the experiments, undrained shear strength was measured at distances of 62.5 mm, 187.5 mm, 312.5 mm, and 437.5 mm from the anode, while water content was measured at the same distances from the anode at depths of 10 mm, 100 mm, and 190 mm. Additionally, undisturbed soil samples were taken from the same locations for scanning electron microscopy
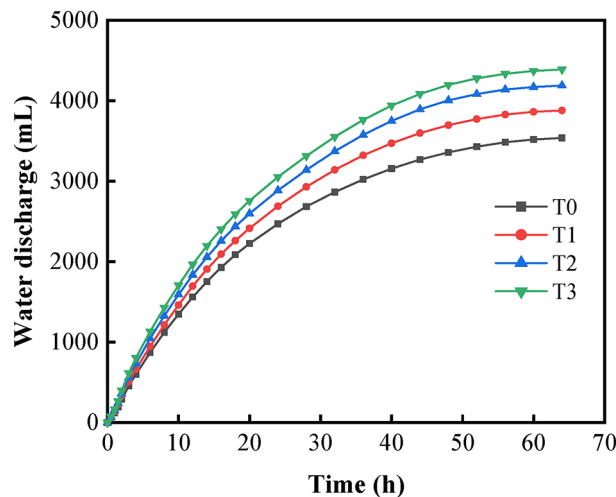
Fig. 2. Variation of drainage volumes with time during treatment for different injection procedures.

(SEM) and mercury intrusion porosimetry (MIP) analysis. Energization should be halted when the drainage rate for all tests falls below 5 mL/h to ensure a consistent energization duration across all four test groups. After the experiments, the undrained shear strength was measured by portable miniature shear vane apparatus at a distance of 62.5 mm, 187.5 mm, 312.5 mm, and 437.5 mm to the anode, and the water content was measured by sampling from the same distance to anode at three different depths of 10 mm,100 mm,190 mm. In addition, undisturbed soil samples were taken at the same locations for SEM and MIP analysis.

Results and discussion
Drainage volume and drainage rate
Drainage volume is the most direct indicator of the effect of electro-osmosis. As shown in Fig. 2, the drainage volume increases progressively over time. At the end of the experiment, the drainage volumes for the T0, T1, T2, and T3 were 3538.41 mL, 3878.92 mL, 4189.83 mL, and 4388.1 mL, respectively. The chemical grouting groups showed increases in drainage volume by 9.62%, 18.41%, and 24.01% compared to the electro-osmosis alone. The comparison of total drainage volumes for T0 through T3 reveals that T1, T2, and T3 all had higher drainage volumes than T0, with T3 exhibiting the greatest volume. This improvement can be attributed to the increased amount of movable cations in the soil, which enhances the drainage process. In the electrochemical groups T1 to T3, Na^+ injected in T1 directly participated in the drainage, whereas Ca^{2+} and Fe^{3+} in T2 and T3 primarily replaced lower-valence cations adsorbed on the soil particle surfaces. These displaced lower-valence cations were converted into hydration cations that more freely migrated and participated in the drainage. Furthermore, the replacement of cations on soil particle surfaces reduces the thickness of the diffusion double layer (DDL), decreases the amount of weakly bound water around the particles, and improves soil water permeability. As the valence of cations increases, the enhancement effect becomes more pronounced, facilitating better drainage of the cathode soil. Consequently, the drainage volumes for T1, T2, and T3 were higher than that of T0.

Figure 3 illustrates the curves of drainage rate over time. According to the figure, the drainage rate for each group is relatively high in the early stages of the test, with an overall upward trend. For each experiment, the drainage rate peaks within the first 3 h, with T1, T2, and T3 showing higher rates than T0, and T3 achieving the highest rate. This indicates that chemical grouting enhances the drainage rate of electro-osmosis when the anions in the solution are consistent, and the effect is more pronounced with higher valence cations. The reason is that the high valence cations have more charge and the ionic strength is greater than the low valence cations. High valence cations, having more charge and greater ionic strength compared to low valence cations, have a more significant impact on electro-osmosis and electrophoresis, thus promoting an improved drainage rate. In the middle of the test, the drainage rates for T2 and T3 decrease rapidly. This is due to the injected high valence cations replacing more low valence cations to participate in drainage, which increases electroosmotic discharge and accelerates the loss of movable cations in the soil. As a result, the drainage rate significantly drops in the middle and late stages of the experiment.

Current
The variation of the current with time is shown in Fig. 4. At the initial stage of the experiment, the current increases the internal temperature of the soil, which decreases the soil resistivity, resulting in a slight increase in current across all groups. As a significant amount of pore water is drained, the current rapidly decreases after reaching its maximum value and gradually stabilizes in the later stage of the experiment. The current of each experimental group was different according to the valence of injected cations. The initial currents for T0, T1, T2, and T3 were 0.71 A, 0.81 A, 1.0 A, and 1.07 A, respectively. Compared to T0, the currents of the T1, T2, and T3 with chemical grouting increased by 14.1%, 40.8%, 50.7%, respectively. The main reason for this difference is that the injection of metal cations, which raises the ion concentration of the soil and reduces its resistivity,
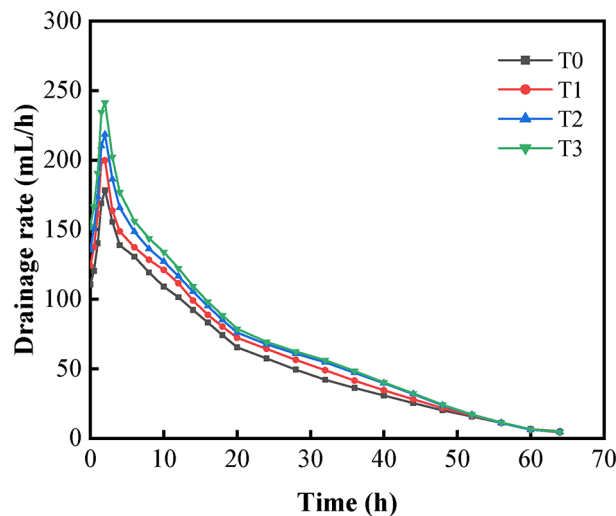
Fig. 3. Variation of drainage rate with time during treatment for different injection procedures.
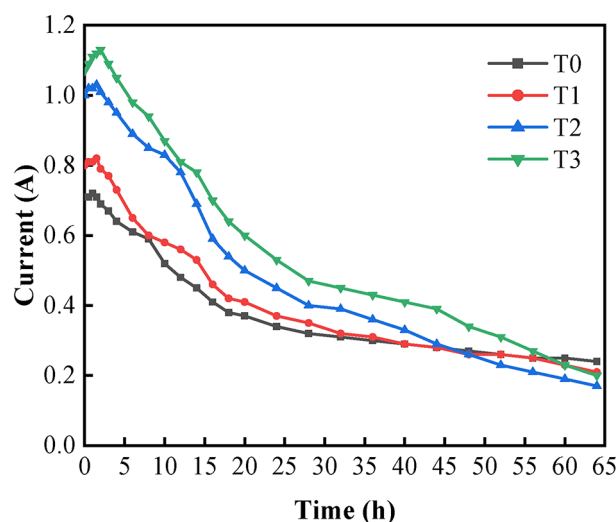

Fig. 4. Variation of current during treatment for different injection procedures.

with higher valence cations having a more pronounced effect. Consequently, the initial currents for T1, T2, and T3 were higher than for T0. During the first 2 h, the current increased to 0.73 A, 0.84 A, 1.03 A, and 1.13 A for T0 through T3, respectively. After this period, the current gradually decreased, with T1, T2, and T3 showing a faster decline than T0. At the end of the test, the currents of each test group are basically the same. By the end of the test, the currents across all groups were similar. As shown in Fig. 3, the change in drainage rate is positively correlated with the rate of current decay. With the progress of electro-osmosis, pore water, and cations are continuously discharged. The improved drainage rates in the electrochemical groups (T1-T3) led to greater early-stage discharge of pore water and cations, significantly reducing soil electrical conductivity. This indicates that while higher valence cations markedly improve the current, they also accelerate the current decay rate in the middle and later stages of the experiment.

Temperature

The temperature changes at different positions of the soil during the test are shown in Fig. 5. The test was carried out at a room temperature of 17 °C. In the first 14 h, the soil temperature increased continuously with the progress of electro-osmosis and then gradually decreased to a stable level. The trend in soil temperature changes is consistent with the current changes. According to Joule's law, the passage of current through the soil generates Joule heat, which raises the soil temperature. Concurrently, the increase in temperature decreases the soil's resistivity, leading to a further increase in current, resulting in a notable rise in soil temperature in the early stages of the test. However, as water electrolysis occurs during electro-osmosis, the generation of H^+ and OH^- ions reduces soil resistivity. As electro-osmosis continues, pore water is expelled from the soil at the cathode,
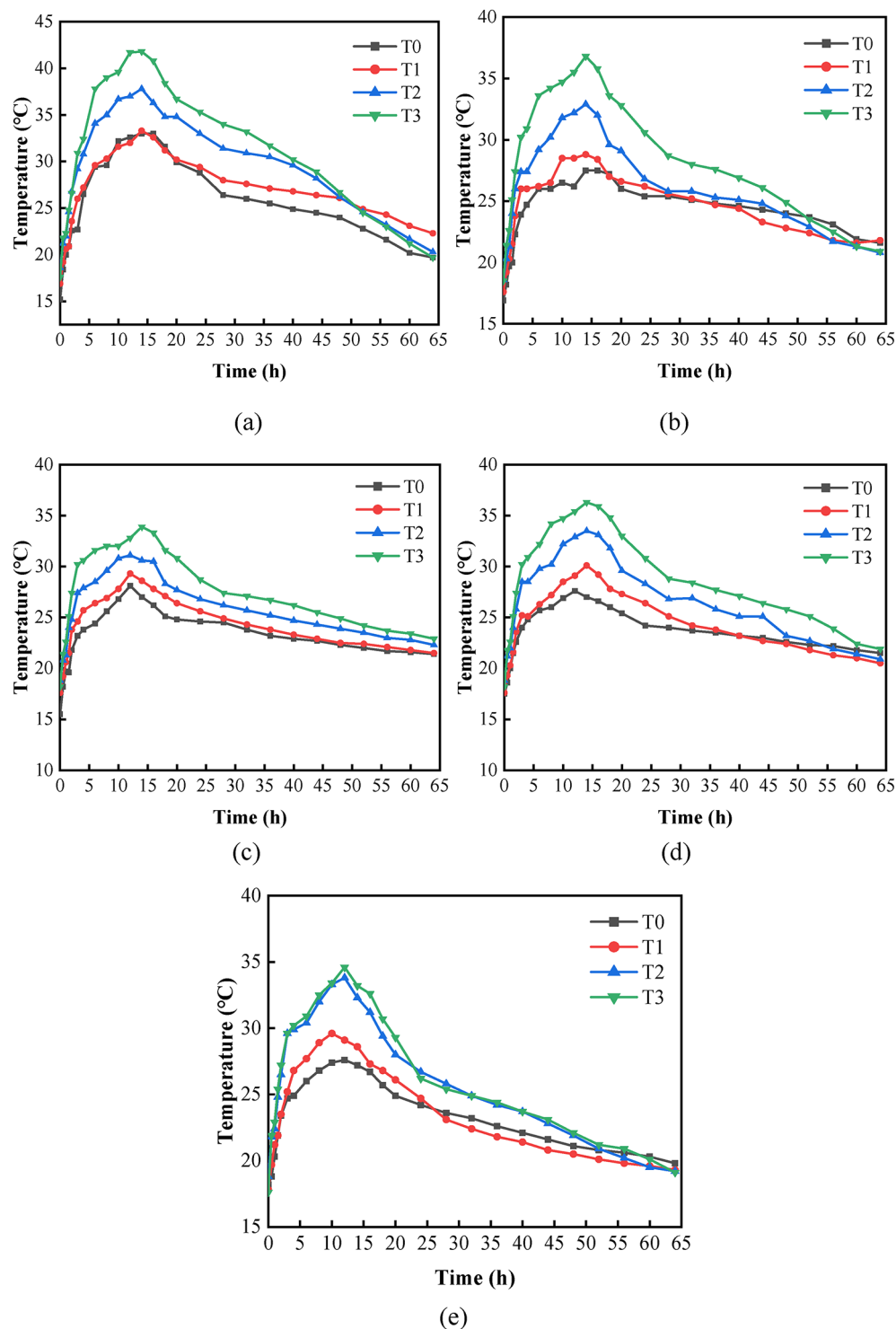
Fig. 5. Curves with soil temperature (**a**) 5mm to anode ,(**b**)125mm to anode, (**c**) 250mm to anode ,(**d**) 375mm to anode, (**e**) 495mm to anode

leading to an increase in soil resistivity. When the rise in resistivity due to soil drainage outweighs the decrease in resistivity from temperature increase and water electrolysis, the current decreases continuously, and the soil temperature gradually stabilizes.

Comparing the temperature curves at each measuring point reveals that the maximum temperature near the anode is the largest. This can be attributed to two main factors. First, the electro-osmotic reinforcement causes pore water near the anode to be transported to the cathode by cations under the influence of the electric field. As a result, the cation and pore water content near the anode decreases rapidly in the early stages, leading to increased resistivity in this region. This higher resistivity generates more Joule heat, causing the temperature near the anode

to be higher than at other positions under the same current[14]. Second, the intensity of electrochemical reactions near the anode produces additional heat, further raising the soil temperature. Consequently, temperatures in T2 and T3, where higher valence cations were used, are higher than those in T1 and T0. However, as the current in T2 and T3 sharply decreased in the later stages, the temperature drop rate also accelerated. By the end of the test, temperatures at the same positions in each test group were similar and slightly higher than before the test.

Electro-osmotic permeability coefficient

The electro-osmotic permeability coefficient (k_e) is one of the basic properties of the soil. Similar to the hydraulic permeability coefficient, the electro-osmotic coefficient of the soil determines the drainage rate of the soil during electro-osmosis. According to the theory of Esrig[24], the electro-osmotic permeability coefficient in the process of electro-osmosis can be expressed by Eq. (1):

$$k_e = \frac{v_e L}{\Delta \phi \, A} \tag{1}$$

Where v_e is the electroosmotic drainage rate, k_e is the electro-osmotic permeability coefficient of the soil, $\Delta \phi$ (V) is the potential difference acting on both ends of the soil, L is the length of the soil, generally considered to be the distance between the cathode and the anode, and A is the cross-sectional area of the soil through which current or water flows. In the equations, L/A is a constant, indicating that the electro-osmotic permeability coefficient is determined by the ratio of the drainage rate over a specific time interval to the effective potential at a given moment, as recorded during the test.

The variation of the electro-osmotic permeability coefficient in the test is shown in Fig. 6. This is derived from Fig. 3 through corresponding calculations and transformations. However, these results are approximate due to measurement errors. The primary sources of error include the calculation of the drainage rate, which is derived by dividing the total drainage volume over a given time interval by the time duration. Moreover, the drained water volume is influenced by electric current and effective potential, and water evaporation may occur due to heat generated within the soil. It can be seen from the curve that the k_e of the soil is consistent with the changing trend of the drainage rate, and there is an obvious peak value. Notably, the higher the valence of cations in the added saline solution, the greater the peak value. This trend is particularly evident during the initial 10 h of electro-osmotic drainage. However, as the electrochemical consolidation process advances, the peak advantage observed in Test T3 gradually diminishes. This phenomenon can be attributed to the high initial drainage rate in T3, which caused a significant amount of cations to be discharged to the cathode along with the water flow. The loss of cations weakened this advantage. Furthermore, the high temperature accelerated water evaporation, leading to a gradual reduction in the drainage rate. Consequently, the electro-osmotic permeability coefficient of the T3 group could not consistently surpass that of the other groups.

However, the k_e calculated using to Eq. (1) represents the average electro-osmotic permeability coefficient of the soil. Throughout the test, hydrated cations migrate from the anode to the cathode under the influence of the electric field, resulting in significant differences in soil properties at different positions by the end of the test. In reality, the electro-osmotic permeability coefficient of the soil near the anode is often lower, which leads to a rapid decline in the drainage rate. Therefore, further research is needed to investigate the evolution of soil electro-osmotic permeability during the electrochemical process.

Water content distribution

The water content distribution of the soil was measured after the test according to the measuring points shown in Fig. 1b. The curves of water content distribution under different cation injection conditions are shown in Fig. 7. It is observed that the water content of the soil gradually increases from the anode to the cathode. This distribution law of water content is consistent with the migrating direction of cations in the electric field, confirming that
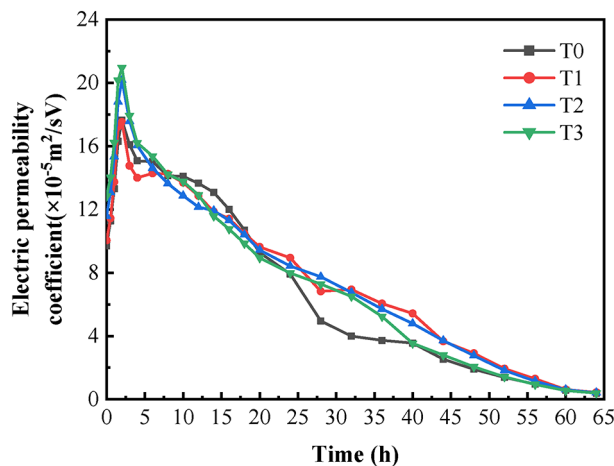
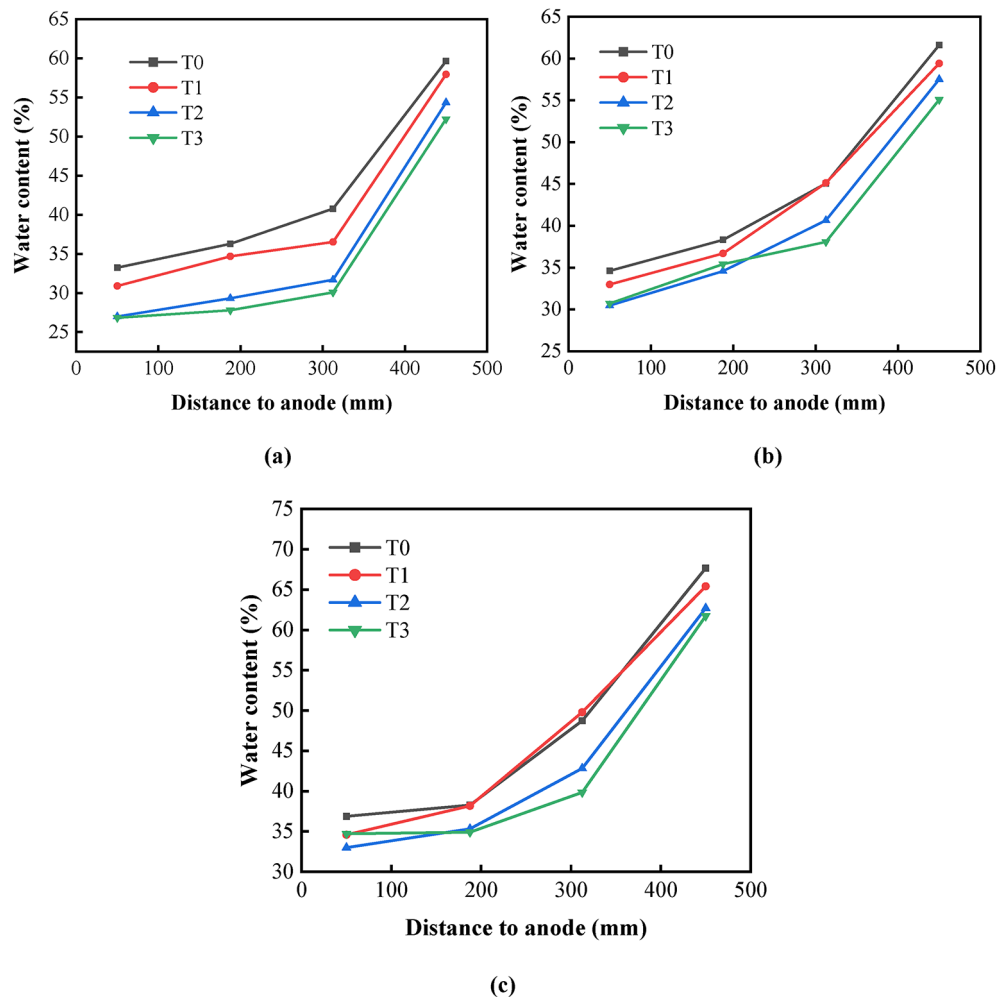**Fig. 6**. Curves with electric permeability coefficient.

Fig. 7. Distribution of average water content after different injection procedures.

electroosmotic drainage mainly involves cations adsorbing water molecules and migrating from the anode to the cathode under the effect of the electric field. In the vertical direction, the surface layer exhibits lower water content compared to the middle and bottom layers. This is because water moves downward under the influence of gravity, resulting in reduced water content at the surface.

The average water content for the surface layer of each test was 42.4, 40.1, 35.6, and 34.2%, for the middle layer was 44.9, 42.6, 40.8, and 39.8%, and for the bottom layer was 48.2, 47.8, 44.2, and 43.6%. This indicates the average water content of the soil in each test decreased by 30–44% compared to the original soil samples. The results show that cation injection promotes a reduction in water content, particularly near the anode and in the middle layers of the soil. The water content decreases with increasing cation valence in the injected solution. The water content after electroosmosis is mainly affected by the drainage volume, and the electrolyzed water reaction during the electroosmosis process also affects the water content. In addition, the current in the soil raises its temperature, thereby promoting water evaporation. Consequently, the increase of the cation valence in the solution has a significant effect on the above factors affecting the water content. In summary, injecting high-valence cation solutions during electrochemical treatment yields better drainage results.

Undrained shear strength

The distribution of undrained shear strength in soil samples after treatment is shown in Fig. 8. When combined with Fig. 7, it is evident that the distribution of shear strength generally corresponds to the water content distribution. The undrained shear strength is lower in the soil near the cathode, where the water content is higher, and higher in the middle and anode areas. This is primarily due to the large amount of pore water near the cathode that remains undrained, leading to a less effective reinforcement.

The results indicate that the injection of the chemical solution has a significant impact on the undrained shear strength of the soil after electro-osmotic treatment. The average undrained shear strength of T1, T2, and T3 increased by 49.1, 99.6, and 112.5%, respectively, compared with T0, demonstrating a notable improvement in soil reinforcement due to the chemical solution. However, the high temperature caused by the injection of high-valence cations during the electro-osmosis process induces small temperature-induced cracks near the anode, which affects the soil's bearing performance. As a result, the undrained shear strength at the anode in
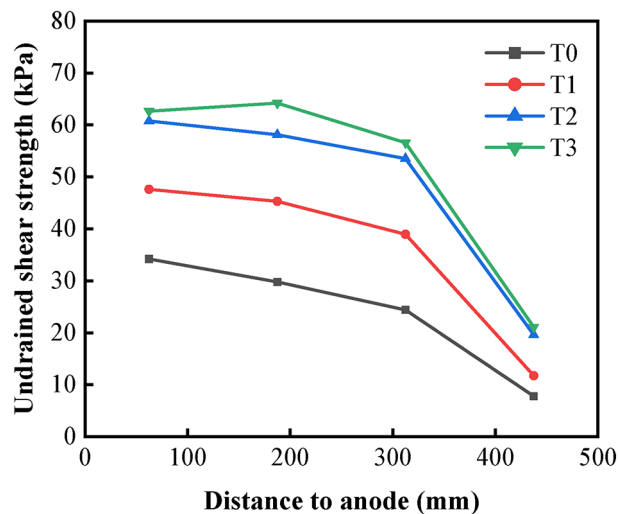
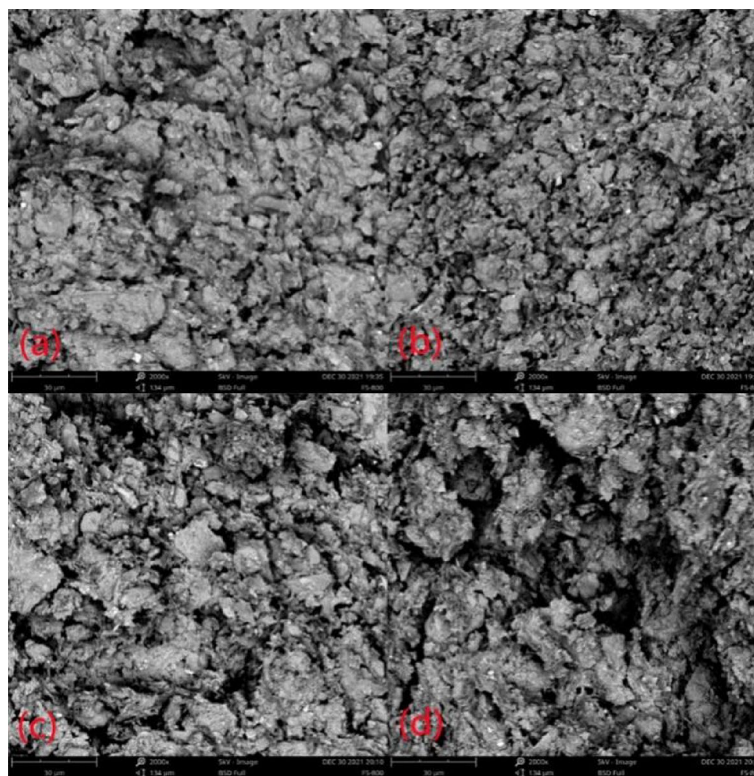**Fig. 8**. Distribution of shear strength different injection procedures.

Fig. 9. SEM image of the microstructure of soil sample before treatment (**a**) T0, (**b**) T1 ,(**c**) T2, (**d**) T3.

T2 and T3 is comparable to that in the middle, with T3 even showing slightly lower shear strength at the anode than in the middle. In addition, due to water electrolysis at the cathode, OH^- ions are produced. In this alkaline environment, Ca^{2+} and Fe^{3+} ions form colloidal hydroxide precipitates, such as calcium hydroxide and iron hydroxide, which effectively fill the voids between soil particles. This process positively contributes to improving the strength of the high-water-content soil in the cathode region.

SEM analysis

The microscopic images of soil samples from each test, injected with different chemical solutions and examined after a set duration, are shown in Fig. 9. The analysis was conducted at 2000x magnification. The images demonstrate that an increase in the valence of cations in the injected salt solution results in a gradual enlargement of soil pore size, more pronounced agglomeration of soil particles, and a loosening of the overall soil structure.

This is primarily due to ion exchange on the surface of soil particles after the addition of cations, which causes the electric double layer to thin and reduces the repulsion between soil particles, leading to flocculation[25].

The SEM images of soil samples at different positions in each test group after the treatment are shown in Figs. 10 and 11. The images of soil samples near the electrode were selected for comparative analysis, and the magnification was 2000 times. As shown in Fig. 10, the soil structure near the anode after treatment is more compact, and the pore volume is significantly reduced. It can be found in Fig. 10b,c,d that the soil after electrochemical reinforcement has smaller cracks near the anode, especially in Fig. 10b,c. When these observations are combined with the data from Figs. 5, 6, 7 and 8, it becomes clear that the main reason is the internal temperature of the soil increases during the electroosmotic treatment process, especially near the anode. The most noticeable temperature changes occur in this region, while the outer surface of the soil remains cooler. These inconsistent temperature changes lead to unsynchronized thermal expansion and contraction of the soil, resulting in small temperature-induced cracks within the soil.

Figure 11 shows the microscopic images of the soil near the cathode of each test. Compared to the soil before treatment, the soil near the cathode after electro-osmosis treatment exhibits a distinct sheet-like structure. During the electroosmosis process, the cations migrate with the pore water to the vicinity of the cathode, accumulating there[23]. This accumulation causes flocculation of the soil near the cathode, leading to an increase in pore size. As a result, more pronounced pores can be observed in Fig. 11b compared to Fig. 11a. Additionally, the hydrolysis reaction creates an alkaline environment near the cathode, where the injected Ca^{2+} and Fe^{3+} ions react with OH^-, forming cementation that fills the soil pores. Consequently, the pores in Fig. 11c,d are smaller compared to those in Fig. 11b.

MIP analysis

The MIP results for different positions of each test group are shown in Figs. 12 and 13. According to the cumulative mercury intrusion results in Fig. 12, the soil pore volume near the anode is smaller than that near the cathode, which corresponds with the distribution of soil shear strength. Among all experiments, T0 exhibited the smallest pore volume, particularly in the NC area. The main reason is that the injected cation adsorbs to the surface of soil particles, which reduces the ζ potential, thins the diffuse double layer (DDL), and decreases the repulsive forces between particles, leading to flocculation and an increase in pore volume[25]. As the progresses of electro-osmosis, the cations migrate towards the cathode under the electric field, causing a significant increase in cation concentration and more obvious flocculation in the soil near the cathode, further increasing pore volume in this region. Figure 12c shows that the total pore volume in T1 was much higher than in T2 and T3, as the Ca^{2+} and Fe^{3+} injected in T2 and T3 chemically reacted in the alkaline environment near the cathode to produce cementation, effectively filling the pores in the soil, resulting in a significantly smaller pore volume in T2 and T3 than T1. However, in Fig. 12d, the differences in pore volume across the tests are less evident, mainly
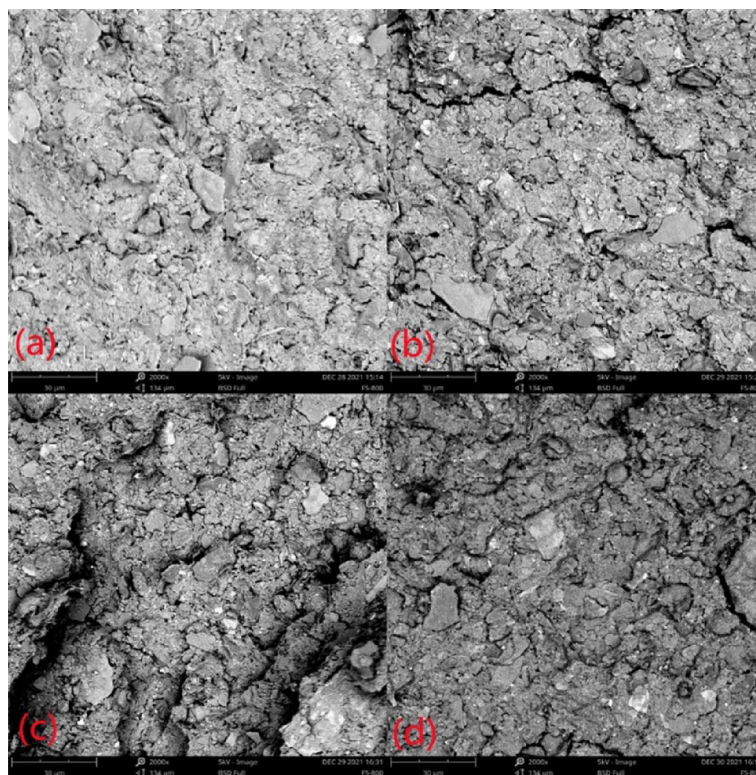

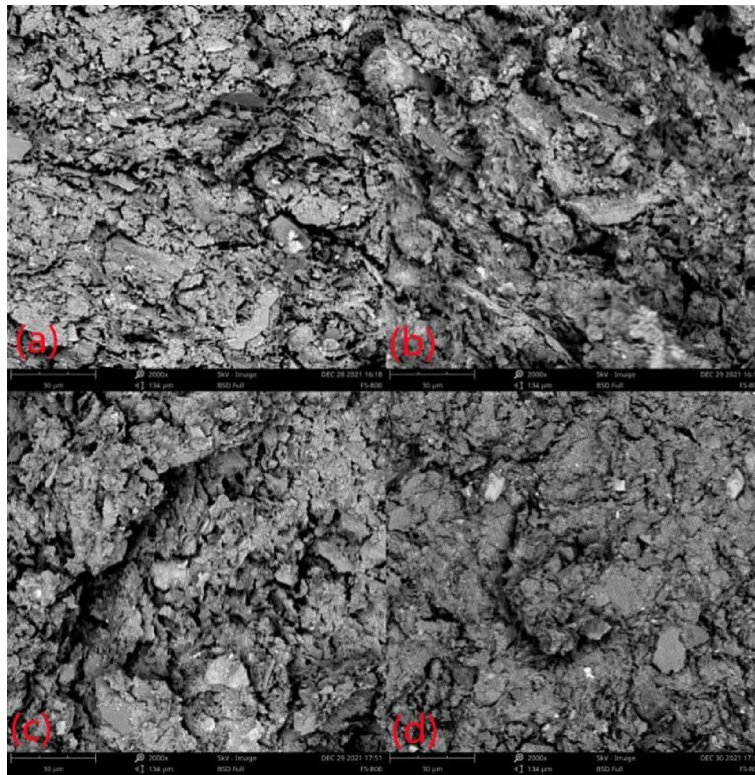**Fig. 10**. SEM image of the microstructure of soil sample near the anode after treatment (**a**) T0, (**b**) T1, (**c**) T2, (**d**) T3.

Fig. 11. SEM image of the microstructure of soil sample near the cathode after treatment (**a**) T0, (**b**) T1, (**c**) T2, (**d**) T3.

due to the high water content in this area, which led to less effective reinforcement and minimal changes in soil pore volume across the groups.

Figure 13 presents the dV/d(logD)-d curve of the soil sample, illustrating the dominant pore diameter distribution. The pore size distribution in the anode area showed minimal change after electrochemical treatment, with the dominant pore size and content across all groups remaining consistent, primarily within the 300–400 nm range. The most significant variations occurred in the NC and CA areas. As shown in Fig. 10c, in the NC area, the dominant pore size varied notably depending on the injected cations, with the sizes recorded as 250 nm, 1450 nm, 450 nm, and 450 nm for each experimental group, respectively. The dominant pore size in T1-T3 is significantly larger than in T0. This increase is due to the higher number of movable cations in the soil, leading to a greater cation concentration in the cathode area, which in turn enlarges the dominant pore size. However, in T2 and T3, the injected Ca^{2+} and Fe^{3+} precipitated through chemical cementation in the alkaline environment near the cathode, reducing the dominant pore size. In contrast, the low-valence cations in T1 did not undergo such reactions, leading to a significant increase in dominant pore size, contributing to uneven reinforcement. Figure 13d shows the pore size distribution of soil in the CA area. The pore size distribution was also affected, with the cation accumulation and undischarged pore water limiting the reinforcement effect. Nonetheless, the injected cations still influenced the soil's pore size. T0 exhibited no clear dominant pore size, with the curve appearing as a plateau. However, with the increase of the cation valence, the pore content of specific pore sizes grew significantly, and the pore size of the soil is mainly about 1000 nm. Finally presents an obvious single-peak curve, indicating that the mineral content of certain particle sizes in the soil sample increases significantly, leading to the increase of the dominant pore size which can improve the soil structure near the cathode to some extent. Overall, while the addition of cations caused flocculation, increasing the pore volume and dominant pore size, particularly in the cathode area, the overall pore distribution became more uniform, and the soil structure was improved. The chemical cementation reaction due to higher valence cations effectively counteracted the increase in pore volume.

Discussion

By studying the influence of different cations in the chemical solutions injected into the soil on the effect of electro-osmotic drainage and consolidation, it was found that the increase in the valence of the cations injected into the soil leads to a better reinforcement effect. The varying valence of the injected cations significantly alters the soil parameters. As shown in Fig. 6, the electro-osmotic coefficient (ke) of the soil treated with chemical solutions increases notably compared to T0. The different valence of injected cations makes the soil parameters change obviously. As observed in Fig. 6, the electro-osmotic coefficient (ke) of soil treated with chemical solutions shows a significant increase compared to T0. The pore volume and dominant pore size of soil increased obviously after treatment in Fig. 12~13. According to the double electrical layer (DEL) theory, the soil surface
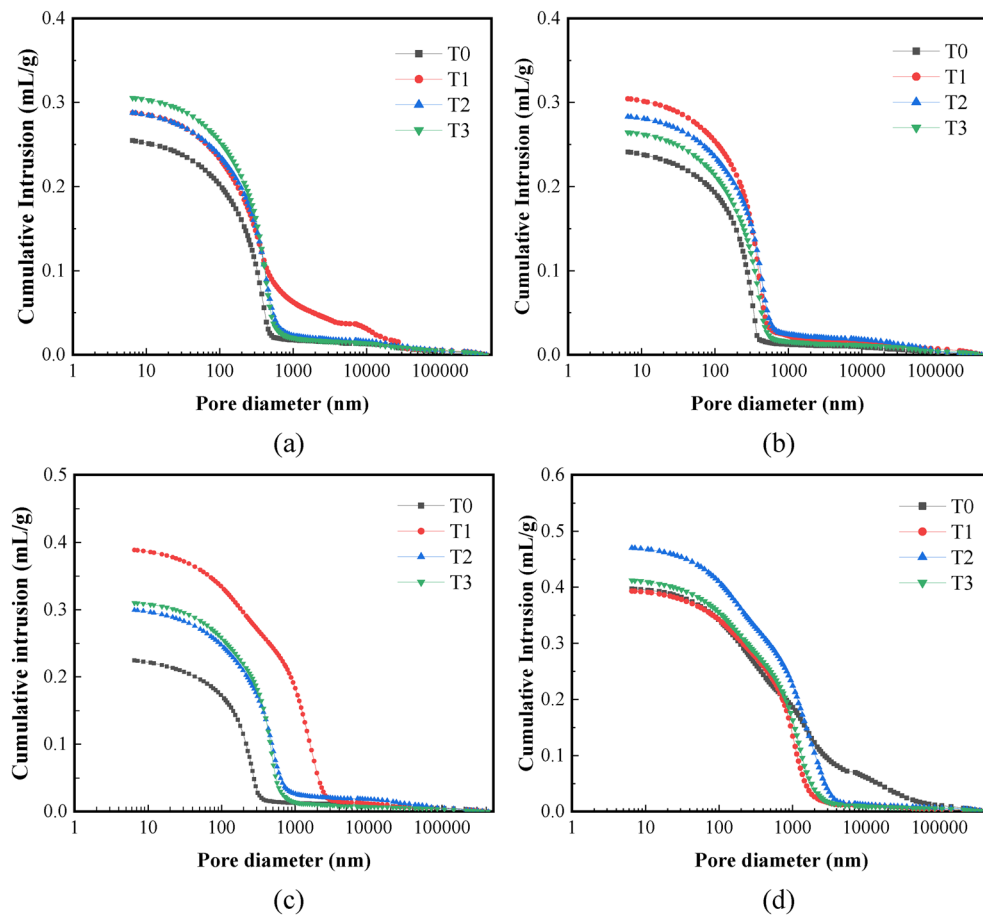
Fig. 12. Cumulative mercury intrusion (**a**) 62.5mm to anode, (**b**) 187.5mm to anode, (**c**) 312.5mm to anode, (**d**) 437.5mm to anode.

carries a negative charge. Under the influence of electrostatic forces, cations in pore water are adsorbed onto the surface of soil particles, neutralizing the negative charges on the soil surface. This process reduces the soil's ζ potential, thins the double diffuse layer (DDL), and increases the soil's electro-osmotic permeability coefficient[25]. The decrease in repulsive forces between soil particles causes fine particles in the clay to aggregate more easily, significantly impacting the soil structure and drainage performance. Thus, changes in the thickness of the DDL have a pronounced effect on electro-osmotic drainage.

In general, the main action channels of electrochemical reinforcement are divided into two channels: promoting drainage and improving soil structure, compared to the traditional electro-osmosis method. The injection of chemical solutions in T1 ~ T3 increased the ion concentration in the soil, significantly improving drainage. For example, the addition of Na^+ ions in T1 resulted in more hydrated sodium ions that migrated freely, thus enhancing drainage compared to T0. High-valence cations, unlike low-valence ones, replace the low-valence cations adsorbed on soil particle surfaces. These high-valence cations neutralize more negative charges on clay particle surfaces, sharply reducing the soil's ζ potential. This reduction thins the diffusion layer, leading to a significant increase in the electro-osmotic coefficient (ke) and drainage rate. Meanwhile, the thickness of the bound water film in the soil becomes thinner, and more bound water is transformed into free water. Under the influence of the electric field, the cations such as Na^+, Ca^{2+}, and Fe^{3+} in the soil migrate toward the cathode, where they are discharged.

Regarding soil structure improvement, the reduction in ζ potential due to cation injection decreases repulsive forces between soil particles, causing fine particles to flocculate into clusters. Although the porosity of soil is slightly increased, the aggregation of fine particles results in a more compact soil structure and optimized pore distribution. In addition, under the effect of DC electric field, some Ca^{2+} and Fe^{3+} ions migrate to the cathode and conducted a chemical cement reaction in the alkaline environment near the cathode. The generated cementation fills the pores caused by flocculation and enhances the integrity of the soil. As a result, the shear strength, pore volume, and overall soil quality of T2 and T3 are superior to those of T1.

Conclusion

In this study, electrochemical experiments were conducted on soft clay using various injected chemical solutions. Based on the analysis of macroscopic parameter changes and microstructure evolution, the following conclusions were drawn:
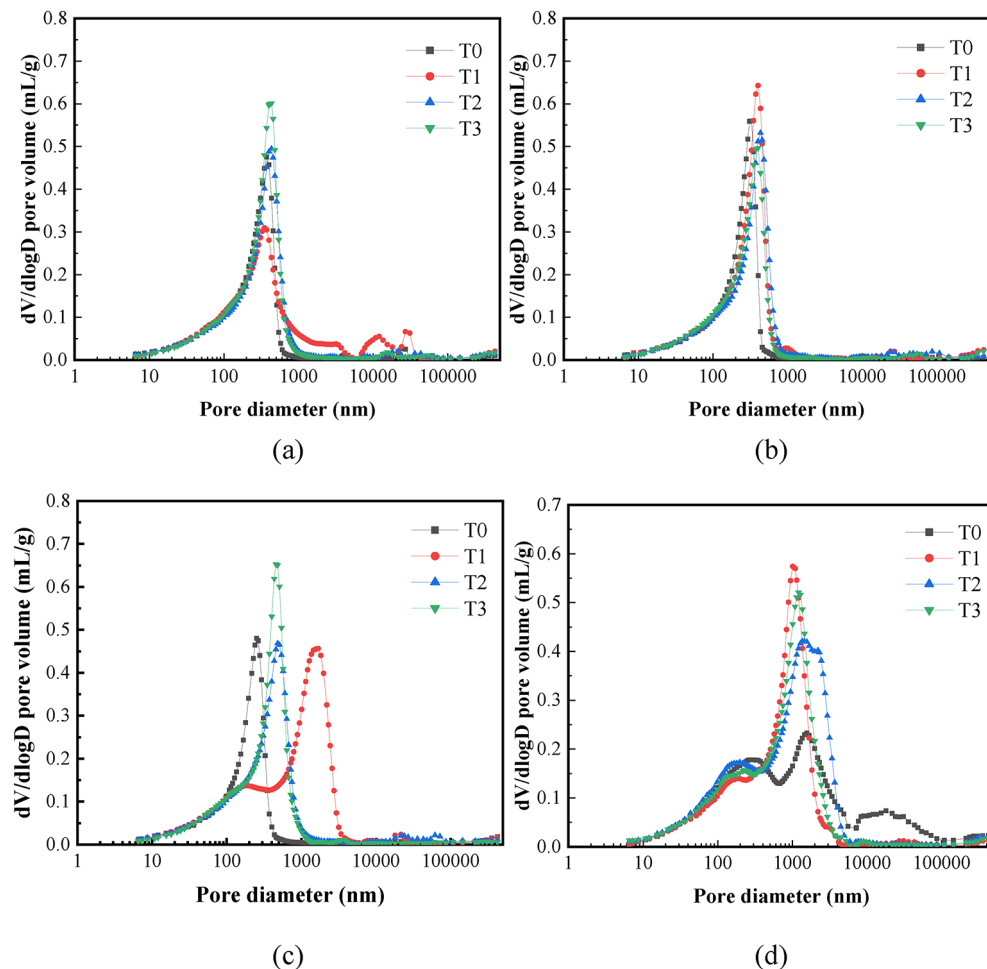
Fig. 13. Pore size diameter distribution (**a**) 62.5mm to anode, (**b**) 187.5mm to anode, (**c**) 312.5mm to anode, (**d**) 437.5mm to anode.

1. The injection of cations significantly increased the current, drainage volume, drainage rate, temperature, and electric permeability coefficient during the initial phase of electrochemical experiments. The shear strength of the soil clearly improved with an increase in the valence of the cation in the injected solution.

2. The electrochemical method notably enhances soil drainage. Injecting cations effectively improves the soil's electric permeability coefficient. An increase in cation valence has a pronounced effect on the soil's ζ potential, leading to a substantial rise in the electric permeability coefficient.

3. The electrochemical reinforcement method also enhances soil structure. Cation injection alters the soil's micro-pore structure, particularly in the cathode area. The decrease in ζ potential and thinning of the diffusion double layer (DDL) lead to the aggregation of fine soil particles, tightening the soil structure. While particle aggregation increases pore volume and dominant pore size, the chemical cementation reactions of Ca^{2+} and Fe^{3+} effectively fill some of these pores, resulting in a better treatment effect compared to low-valence cations.

4. Among all test groups (T0–T3), the injection of $FeCl_3$ achieved the best reinforcement effect. This indicates that high-valence cations have a more pronounced positive impact on the electrochemical method. Therefore, high-valence cations should be preferred in practical engineering applications.

5. For practical engineering use, the electrochemical method for strengthening soft clay foundations can be implemented by drilling injection holes between the cathode and anode. Chemical reagents are then injected into the soil under controlled pressure using an injection probe. By managing the injection pressure and the probe advancement rate, the injection radius can be adjusted, and drainage in the cathode region can be regulated separately.

Data availability
The datasets used and/or analysed during the current study available from the corresponding author on reasonable request.

References

1. Jones, C. J., Lamont-Black, J. & Glendinning, S. Electrokinetic geosynthetics in hydraulic applications. *Geotext. Geomembr.* **29** (4), 381–390. https://doi.org/10.1016/J.GEOTEXMEM.2010.11.011.(2011)
2. Mitchell, J. K. & Soga, K. Fundamentals of soil behavior (Vol. 3, p. USA). New York: John Wiley & Sons. (2005).
3. Micic, S. *Electrokinetic strengthening of soft marine sediments* (Faculty of graduate studies, University of Western Ontario, 1998).
4. Lo, K. Y. & Ho, K. S. The effects of electroosmotic field treatment on the soil properties of a soft sensitive clay. *Can. Geotech. J.* **28** (6), 763–770. https://doi.org/10.1139/t91-093 (1991).
5. Casagrande, I. L. Electro-osmosis in soils. *Geotechnique* **1** (3), 159–177. https://doi.org/10.1680/geot.1949.1.3.159 (1949).
6. Alshawabkeh, A. N., Sheahan, T. C. & Wu, X. Coupling of electrochemical and mechanical processes in soils under DC fields. *Mech. Mater.* **36** (5-6), 453–465. https://doi.org/10.1016/S0167-6636(03)00071-1 (2004).
7. Chien, S. C., Ou, C. Y. & Lo, W. W. Electro-osmotic chemical treatment of clay with interbedded sand. *P I Civil Eng-Geotec.* **167** (1), 62–71. https://doi.org/10.1680/geng.11.00076 (2014).
8. Acar, Y. B. & Alshawabkeh, A. N. Principles of electrokinetic remediation. *Environ. Sci. Technol.* **27** (13), 2638–2647 (1993).
9. Chien, S. C., Ou, C. Y. & Wang, M. K. Injection of saline solutions to improve the electro-osmotic pressure and consolidation of foundation soil. *Appl. Clay Sci.* **44** (3–4), 218–224. https://doi.org/10.1016/j.clay.2009.02.006.((2009).
10. Bjerrum, L., Moum, J. & Eide, O. Application of electro-osmosis to a foundation problem in a Norwegian quick clay. *Geotechnique* **17** (3), 214–235. https://doi.org/10.1680/geot.1968.18.2.276.((1967).
11. Shang, J. Q., Mohamedelhassan, E. & Ismail, M. Electrochemical cementation of offshore calcareous soil. *Can. Geotech. J.* **41** (5), 877–893. https://doi.org/10.1139/t04-030 (2004).
12. Otsuki, N., Yodsudjai, W. & Nishida, T. Feasibility study on soil improvement using electrochemical technique. *Constr. Build. Mater.* **21** (5), 1046–1051. https://doi.org/10.1016/j.conbuildmat.2006.02.001 (2007).
13. Li, X. et al. Effect of electrochemical treatment on consolidation of soft clay. *Geomech. Eng.* **21** (4), 957–964. https://doi.org/10.12989/gae.2018.15.4.957 (2018).
14. Xue, Z. et al. Mechanism of electro-osmotic chemical for clay improvement: Process analysis and clay property evolution. *Appl. Clay Sci.* **166**, 18–26. https://doi.org/10.1016/j.clay.2018.09.001.((2018).
15. Chien, S. C., Ou, C. Y. & Wang, Y. H. Soil improvement using electroosmosis with the injection of chemical solutions: laboratory tests. *J. Chin. Inst. Eng.* **34** (7), 863–875. https://doi.org/10.1080/02533839.2011.591915.((2011).
16. Liu, F. et al. Influence of soluble salt on electro-osmotic consolidation of soft clay. *Soil. Mech. Found. Eng.* **54**, 49–55. https://doi.org/10.1007/s11204-017-9432-x (2017).
17. Ou, C. Y., Chien, S. C. & Wang, Y. G. On the enhancement of electroosmotic soil improvement by the injection of saline solutions. *Appl. Clay Sci.* **44** (1–2), 130–136. https://doi.org/10.1016/j.clay.2008.12.014.((2009).
18. Pączkowska, B. Electroosmotic introduction of methacrylate polycations to dehydrate clayey soil. *Can. Geotech. J.* **42** (3), 780–786. https://doi.org/10.1139/T05-008 (2005).
19. Ou, C. Y., Chien, S. C., Yang, C. C. & Chen, C. T. Mechanism of soil cementation by electroosmotic chemical treatment. *Appl. Clay Sci.* **104**, 135–142. https://doi.org/10.1016/j.clay.2014.11.020 (2015).
20. Chien, S. C., Teng, F. C. & Ou, C. Y. Soil improvement of electroosmosis with the chemical treatment using the suitable operation process. *Acta Geotech.* **10**, 813–820. https://doi.org/10.1007/s11440-014-0319-y (2015).
21. Ge, S., Zang, J., Wang, Y., Zheng, L. & Xie, X. Combined stabilization/solidification and electroosmosis treatments for dredged marine silt. *Mar. Georesour Geotechnol.* **39** (10), 1157–1166. https://doi.org/10.1080/1064119X.2020.1817205.((2021).
22. Korolev, V. A. & Nesterov, D. S. Influence of electro-osmosis on physicochemical parameters and microstructure of clay soils. *J. Environ. Sci. Heal A.* **54** (6), 500–571. https://doi.org/10.1080/10934529.2019.1571321.((2019).
23. Mahalleh, H. A. M., Siavoshnia, M. & Yazdi, M. Effects of electro-osmosis on the properties of high plasticity clay soil: Chemical and geotechnical investigations. *J. Electroanal. Chem.* **880**, 114890. https://doi.org/10.1016/j.jelechem.2020.114890.((2021).
24. Esrig, M. I. Pore pressures, consolidation, and electrokinetics. *J. Soil. Mech. Found. Div.* **94** (4), 899–921 (1968).
25. Chai, J. C., Shen, S. L. & Geng, X. Effect of initial water content and pore water chemistry on intrinsic compression behavior. *Mar. Georesour Geotechnol.* **37** (4), 417–423. https://doi.org/10.1080/1064119X.2018.1445146.((2019).

Acknowledgements

Author contributions

Guohui Yuan: Funding acquisition; Validation; Writing - Review & EditingXiaomeng Cao: Writing - Review & EditingZiyang Gao: Formal analysis.Junfeng Ni: Validation.Xiaobing Li: Funding acquisition; Writing - Review & EditingHongtao Fu: MethodologyJianqi Wu: Data analysis and WritingChenyang Zhou: Data analysis and Writing.

Declarations

Competing interests

The authors declare no competing interests.

Additional information

Correspondence and requests for materials should be addressed to X.L.

Reprints and permissions information is available at www.nature.com/reprints.

Publisher's note Springer Nature remains neutral with regard to jurisdictional claims in published maps and institutional affiliations.